

Raman scattering by spin excitations in α -MnSe

A. Milutinović, N. Tomić, S. Dević, P. Milutinović, and Z. V. Popović

Center for Solid State Physics and New Materials, Institute of Physics, Pregrevica 118, 11080 Belgrade/Zemun, Yugoslavia

(Received 27 February 2002; published 28 June 2002)

Raman spectra of polycrystalline α -MnSe were measured in the temperature range from 17 to 100 K. We found a peak at 18 cm^{-1} at low temperatures that shifts to lower frequencies when the temperature increases. From frequency vs temperature dependence we assigned it as one magnon mode at $\mathbf{k}=0$. The magnon dispersion relations were calculated using random phase Green function approximation. The exchange energies were estimated. The Néel temperature was determined by fitting the $\omega_{1M}(T)/\omega_{1M}(0)=f(T/T_N)$ dependence with the experimental data.

DOI: 10.1103/PhysRevB.66.012302

PACS number(s): 78.30.Fs, 71.36.+c, 75.30.Ds, 75.50.Ee

I. INTRODUCTION

Recently, manganese oxides and chalcogenides have attracted considerable attention because of a large variety of optical, magnetic, and transport properties, which hold the promise of realizing spintronic devices.¹ Among the $3d$ transition-metal chalcogenides MnS, MnSe, and MnTe are antiferromagnetic (AFM) compounds with respective Néel temperatures T_N of 152,² 124,³ and 307 K.⁴ In the case of MnS and MnSe, the stable crystal structure is cubic, NaCl type (α phase), whereas the MnTe crystallizes in the hexagonal NiAs-type structure. They can also be stabilized artificially in the zinc blende (β phase) structure by epitaxial growth or by alloying with II-VI semiconductors.⁵ In the case of α -MnSe the second phase with hexagonal NiAs crystal structure arises at about 190 K. The NiAs structure of MnSe consists of ferromagnetic sheets, stacked antiferromagnetically perpendicular to the \mathbf{c} axis. The number and size of the NiAs bands increase with decreasing of temperature and may occupy 15–38 % of crystal volume.³ On warming, the NiAs modification converts to the cubic form and completely vanishes at 300 K staying magnetic up to this temperature. Because of that some of magnetic and neutron diffraction measurements were contradictory interpreted.^{6–10} The cubic form itself exhibits AFM-II (Ref. 5) spin ordering, Fig. 1, with the Néel temperature of 122 K, according to Ref. 3, or between 130 and 250 K, due to thermal hysteresis and sample history effects, as it was referred by other authors.^{6–8}

Optical properties of α -MnSe are investigated by far-infrared reflectivity,¹¹ without any evidence of presence of the NiAs phase in α -MnSe. Optical phonons are Raman inactive in the paramagnetic phase of the α -MnSe. To the best of our knowledge the Raman scattering in the AFM phase of α -MnSe has not been published until now.

In this work we prepared polycrystalline α -MnSe samples by sintering technique and investigated them by Raman spectroscopy. The one-magnon mode at 18 cm^{-1} is found in the Raman spectra recorded at 17 K. This mode shifts to lower frequencies when the temperature increases. We developed a simple model for AFM state of MnSe and calculated the magnon dispersion branches using the random phase Green function approximation (RPGA). The exchange parameters were estimated by comparison theoretical with experimental results. The Néel temperature $T_N=90 \text{ K}$ was de-

termined by fitting the $\omega_{1M}(T)/\omega_{1M}(0)=f(T/T_N)$ dependence.

II. EXPERIMENT

Polycrystalline samples of α -MnSe were made by sintering. Stoichiometric amounts of Mn and Se powders were properly mixed and heated at 930°C in a sealed evacuated quartz tube for seven days. The product was ground and pressed into pellets (diameter 12 mm, thickness 1 mm) under the pressure of 70 MPa. The quality of α -MnSe samples was checked by x-ray diffractometry. No tracks of starting elements or impurity phases (MnSe_2) confirm a good quality of the samples.

Raman spectra of α -MnSe were excited by 514.5 nm line of an Ar-ion laser, focused to a line focus using a cylindrical lens in order to avoid the sample heating. The scattered light

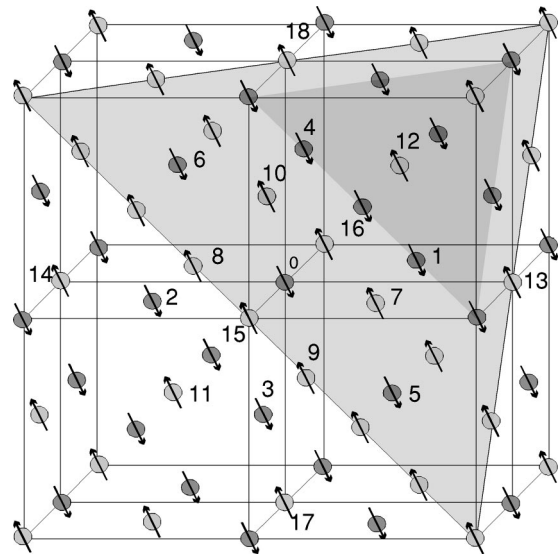


FIG. 1. Face-centered-cubic (fcc) lattice of α -MnSe (NaCl type). In the antiferromagnetic phase of α -MnSe the spins of manganese ions are aligned in (111) sheets. The direction of magnetic moment of the magnetic ion in each lattice point is indicated by an arrow. (1–12). The nearest-neighbor and (13–18) the next-nearest-neighbor ions.

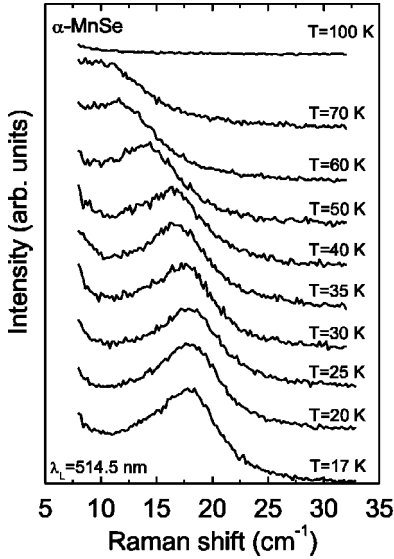


FIG. 2. Unpolarized Raman spectra of α -MnSe at various temperatures recorded in the spectral range from 6 to 33 cm^{-1} .

was dispersed by Jobin-Yvon U 1000 monochromator and detected using conventional photon-counting system. The laser line power was 30 mW. Low-temperature spectra were measured using Leybold closed-cycle helium cryostat.

III. RESULTS AND DISCUSSION

Figure 2 shows the unpolarized Raman spectra of α -MnSe measured in the spectral range between 6 and 33 cm^{-1} at temperatures below 100 K. The mode at about 18 cm^{-1} is clearly observed at lowest temperature. This mode shows a strong frequency and intensity change by increasing the temperature. Based on its temperature dependence we assign this mode to scattering by magnons in the AMF phase of α -MnSe at $\mathbf{k}=0$. The similar structure (one-magnon mode) is also observed in diluted magnetic system CdMnTe.^{12,13}

We assume that the α -MnSe exhibits the AFM fcc uniaxial type-II spin structure such as α -MnS (Ref. 14) with magnetic space group $Cc2/c$. Taking into account that uniaxial model for α -MnS gives very good values for magnon frequencies¹⁴ or magnetization¹⁵ we started our consideration with the assumption that the uniaxial model can be applicable on α -MnSe, too. In the case of the NaCl structure, the anions lie on the edges of the cubic fcc cell (Fig. 1) between the second-nearest magnetic neighbors. As a result, the next-nearest-neighbor (NNN) interaction ($J_{\text{NNN}}=J_2$) is usually stronger than the nearest-neighbor (NN) interaction ($J_{\text{NN}}=J_1$). The magnetic anisotropy energy is expected to be mainly of dipolar origin and very small compared to the isotropic exchange energy. The distortion which accompanies AFM ordering can be neglected in the first approximation.

The Hamiltonian to be considered is the sum of single-ion Hamiltonians in the form

$$\mathcal{H} = J_1^- \sum_{i,j} \vec{S}_i \vec{S}_j + J_1^+ \sum_{i,j} \vec{S}_i \vec{S}_j + J_2 \sum_{i,j} \vec{S}_i \vec{S}_j + \sum_i (D_1 S_{x_i}^2 + D_2 S_{y_i}^2), \quad (1)$$

where the summation goes over all nearest and next-nearest neighbors; J_1^+ , J_1^- , and J_2 refer to the exchange parameters between nearest neighbors on opposite sublattices, the same sublattice, and next-nearest neighbors, respectively. D_1 describes the anisotropy which restricts the spins to (111) plane (“out-of-plane anisotropy”), and $D_2 (< D_1)$ constrains the spins to particular direction within this plane (“in-plane anisotropy”). Here we neglected contraction and distortion of lattice in antiferromagnetic phase and put $J_1^+ = J_1^- = J_1$. After applying the Holstein-Primakoff transformation and the standard diagonalization procedure we obtain the eigenvalues in the form

$$\hbar \omega_{1(2)\vec{k}} = S \sqrt{(\beta_1 \pm \gamma)(\beta_2 \mp \gamma)}. \quad (2)$$

Quantities $\beta_1 + \gamma$ and $\beta_2 - \gamma$ are defined as

$$\beta_1 + \gamma = 4J_1(c_1c_2 + c_2c_3 + c_3c_1) + 4J_2(c_1^2 + c_2^2 + c_3^2) + 2D_1, \quad (3)$$

$$\beta_2 - \gamma = 4J_1(s_1s_2 + s_2s_3 + s_3s_1) + 4J_2(s_1^2 + s_2^2 + s_3^2) + 2D_2, \quad (4)$$

where c_i and s_i are $c_i = \cos(ka_i)$; $s_i = \sin(ka_i)$, $i = x, y, z$.

Resonant antiferromagnetic energies, when $T \rightarrow 0$ K, are

$$\hbar \omega_{1(2)0} = S \sqrt{24D_{2(1)}(J_1 + J_2)}. \quad (5)$$

The values of J_1 , J_2 , D_1 , and D_2 should be evaluated on the basis of different experimental results. Generally, there are two branches of spin-wave oscillations, therefore for estimating of D_1 and D_2 it is necessary to measure two different resonant antiferromagnetic frequencies at $\vec{k}=0$. In our Raman experiment only one frequency is registered. It means that D_2 is approximately equal to zero as in α -MnS. The other possibility is that two degenerate magnon branches exists with $D_2 = D_1$. The form and the number of dispersion branches can be definitively determined by neutron scattering. By Raman spectroscopy we obtain the value of magnon frequency in $\vec{k}=0$, and that helps enough in estimating values of J_1 , J_2 , and D_1 . Taking $J_1/J_2 = 0.6$,^{7,8} the $\vec{k}=0$ resonant frequency $\omega_0 = 18 \text{ cm}^{-1}$ (Fig. 2), and values $D_1 = 0.236 \text{ cm}^{-1}$ and $D_2 \approx 0$ such as for α -MnS,^{14,15} we obtained $J_1 = 3.375 \text{ cm}^{-1}$ and $J_2 = 5.625 \text{ cm}^{-1}$. Calculated magnon dispersion branches in α -MnSe for three high symmetry directions of \mathbf{k} are presented in Fig. 3.

Confirmation that selected values for J_1 and J_2 are correctly evaluated comes from the agreement between the Néel temperature which is the result of fitting a theoretically found function $\omega/\omega_0 = f(T/T_N)$ in which J_1 and J_2 are included, and independently ordered value of T_N . The ratio ω/ω_0 of magnon frequencies at certain temperature $T (< T_N)$ and $T \approx 0$ K is equal to the ratio of sublattice magnetization at

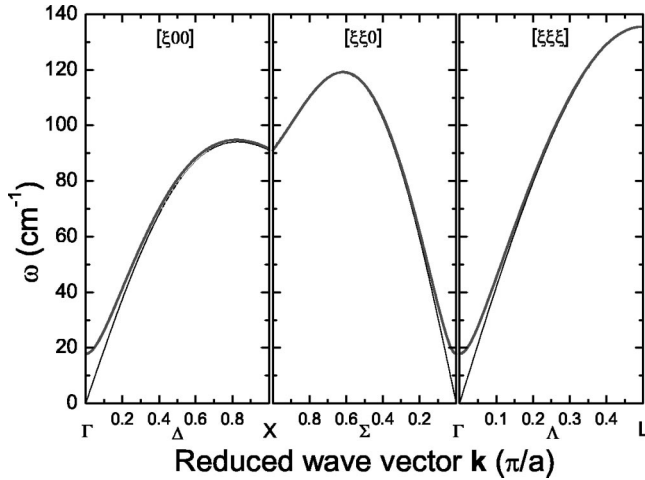


FIG. 3. Magnon dispersion branches in α -MnSe calculated for three high symmetry directions of the wave vector \mathbf{k} .

these temperatures $\omega/\omega_0 \cong M/M_0$.^{15,16} The temperature dependence of the magnon frequency ratio $\omega/\omega_0 = f(T/T_N)$ is obtained on the basis of the random-phase Green's function approximation¹⁵

$$\omega/\omega_0 \cong M/M_0 = \bar{S}/S = B_S(2S \coth^{-1}x); S = 5/2, \quad (6)$$

where B_S is Brillouin function and x :

$$x = \left\langle \frac{\mu}{\sqrt{\mu^2 - \lambda^2}} \coth \left[\frac{\bar{S} \sqrt{\mu^2 - \lambda^2}}{2kT} \right] \right\rangle_{\mathbf{k}}. \quad (7)$$

Quantities $\mu \pm \lambda$ are related with previously defined β_1 and γ as $\mu \pm \lambda = \beta_{1(2)} \pm \gamma - 2D_{1(2)}$ with substituted values for J_1 and J_2 used for estimation of dispersion relations. The best agreement between theoretical calculation, Eq. (6), and experimental data (Fig. 4) was achieved with $T_N = 90$ K. The agreement of these data confirms that evaluated values of exchange integrals, as well as the value of T_N found by

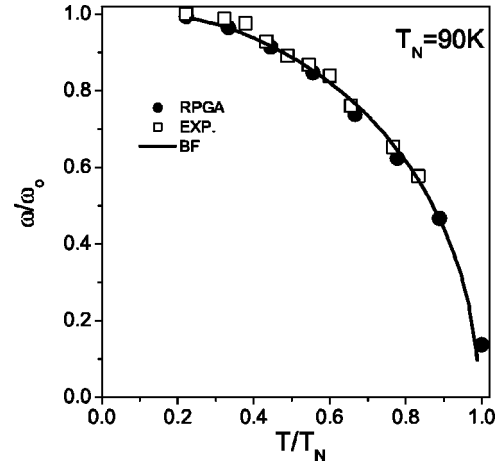


FIG. 4. Temperature dependence of the zero-field one-magnon frequency plotted on a reduced scale. Squares represent measured values; circles are values calculated in the random-phase Green's function approximation (RPGA); line represents the Brillouin function (BF) values calculated for $S = 5/2$.

fitting procedure, are optimally chosen. The antiferromagnetic ordering temperature of our samples is lower than the values found earlier by susceptibility measurements.^{7,8} Difference could be a consequence of different sample quality, as well as different participation of NiAs-phase in the α -MnSe structure.

In conclusion, we have measured Raman scattering in the α -MnSe in the antiferromagnetic phase and found the one-magnon mode at 18 cm^{-1} at 17 K . We calculated the magnon dispersion branches on the basis of simple model and estimated the exchange energies of $J_{1(NN)} = 3.375 \text{ cm}^{-1}$, $J_{2(NNN)} = 5.625 \text{ cm}^{-1}$, and the anisotropy parameter $D_1 = 0.236 \text{ cm}^{-1}$.

ACKNOWLEDGMENTS

This work was supported by Serbian Ministry of Science and Technology under Project No. 1469.

¹S. A. Wolf, D. D. Awschalom, R. A. Buhrman, J. M. Daughton, S. von Molnár, M. L. Roukes, A. Y. Chtchelkanova, and D. M. Treger, *Science* **294**, 1488 (2001).

²D. R. Huffman and R. L. Wild, *Phys. Rev.* **118**, 526 (1966).

³R. J. Pollard, V. H. McCann, and J. B. Ward, *J. Phys. C* **16**, 345 (1983).

⁴K. Ozawa, S. Anzai, and Y. Hamaguchi, *Phys. Lett.* **20**, 132 (1966).

⁵P. Klosowski, T. M. Giebultowicz, J. J. Rhyne, N. Samarth, H. Luo, and J. Furdyna, *J. Appl. Phys.* **69**, 6109 (1991).

⁶R. Lindsay, *Phys. Rev.* **84**, 569 (1951).

⁷J. J. Baniewicz, R. F. Haidelberg, and A. H. Luxem, *J. Phys. Chem.* **65**, 615 (1961).

⁸P. W. Anderson, *Phys. Rev.* **79**, 705 (1950).

⁹A. F. Andersen and H. Rotterud, *Acta Crystallogr., Sect. A: Cryst. Phys., Diffr., Theor. Gen. Crystallogr.* **25**, S250 (1969).

¹⁰A. J. Jacobson and B. E. F. Fender, *J. Chem. Phys.* **52**, 4563 (1970).

¹¹D. L. Decker and R. L. Wild, *Phys. Rev. B* **4**, 3425 (1971).

¹²S. Venugopalan, A. Petrou, R. R. Galazka, A. K. Ramdas, and S. Rodriguez, *Phys. Rev. B* **25**, 2681 (1982).

¹³A. K. Ramdas and S. Rodriguez, in *Diluted Magnetic Semiconductors*, Vol. 25 of *Semiconductors and Semimetals*, edited by Y. K. Furdyna and J. Kossut (Academic, Boston, 1988).

¹⁴H-h. Chou and H. Y. Fan, *Phys. Rev. B* **13**, 3924 (1976).

¹⁵M. E. Lines and E. D. Jones, *Phys. Rev.* **139**, A1313 (1965).

¹⁶M. E. Lines, *Phys. Rev.* **139**, A1304 (1965).